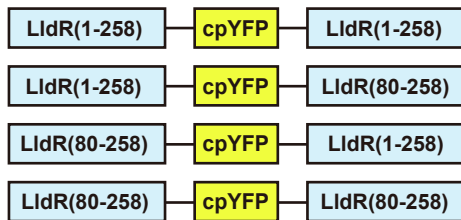


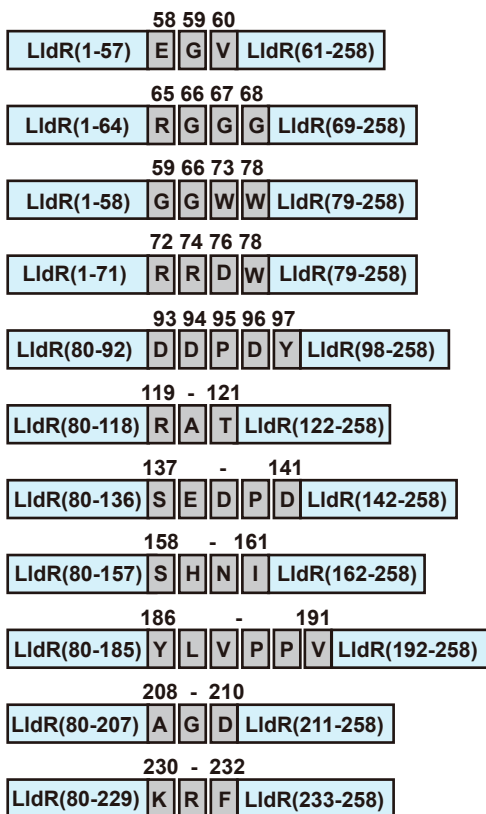
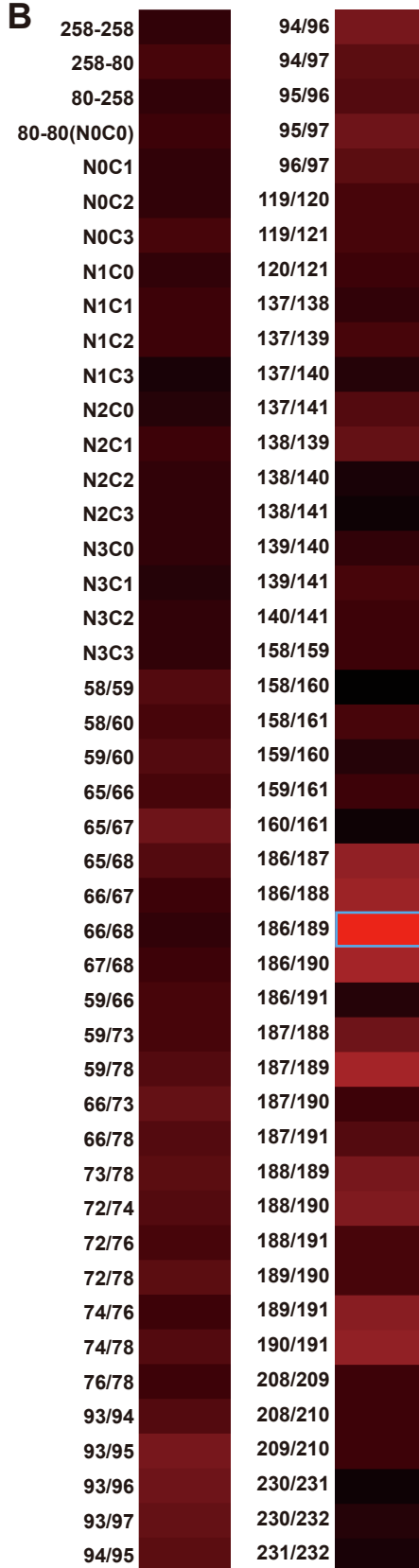
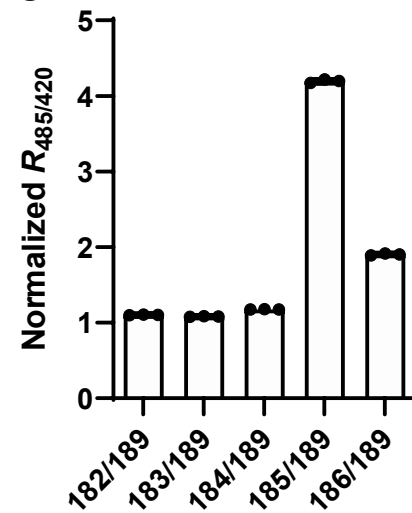
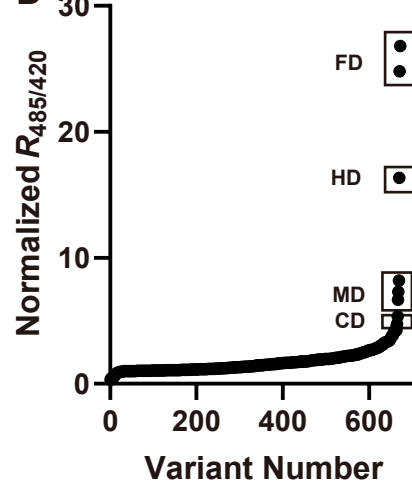
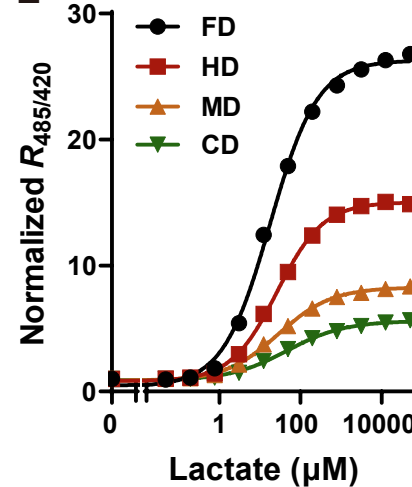
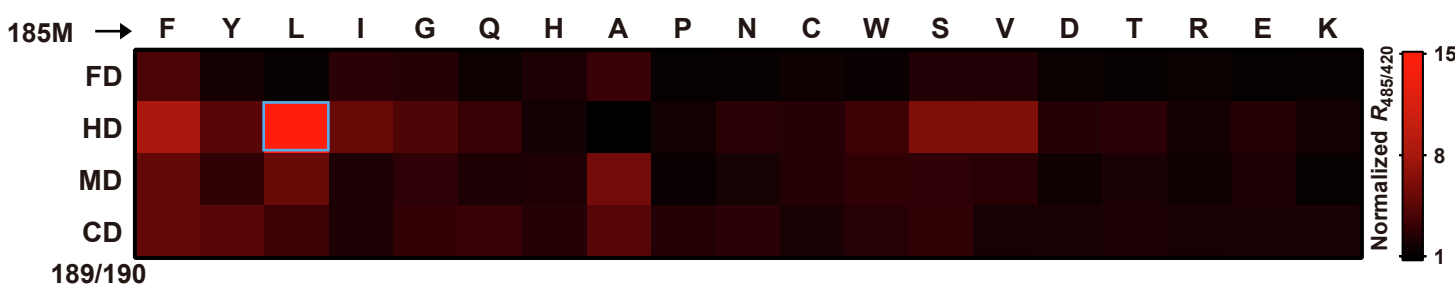
Supplemental information

**Ultrasensitive sensors reveal
the spatiotemporal landscape of lactate
metabolism in physiology and disease**

Xie Li, Yinan Zhang, Lingyan Xu, Aoxue Wang, Yejun Zou, Ting Li, Li Huang, Weicai Chen, Shuning Liu, Kun Jiang, Xiuze Zhang, Dongmei Wang, Lijuan Zhang, Zhuo Zhang, Zeyi Zhang, Xianjun Chen, Wei Jia, Aihua Zhao, Xinfeng Yan, Haimeng Zhou, Linyong Zhu, Xinran Ma, Zhenyu Ju, Weiping Jia, Congrong Wang, Joseph Loscalzo, Yi Yang, and Yuzheng Zhao

A

N0C0	None	None
N0C1	None	G
N0C2	None	GG
N0C3	None	GGG
N1C0	G	None
N1C1	G	G
N1C2	G	GG
N1C3	G	GGG
N2C0	GG	None
N2C1	GG	G
N2C2	GG	GG
N2C3	GG	GGG
N3C0	GGG	None
N3C1	GGG	G
N3C2	GGG	GG
N3C3	GGG	GGG

**B****C****D****E****F**

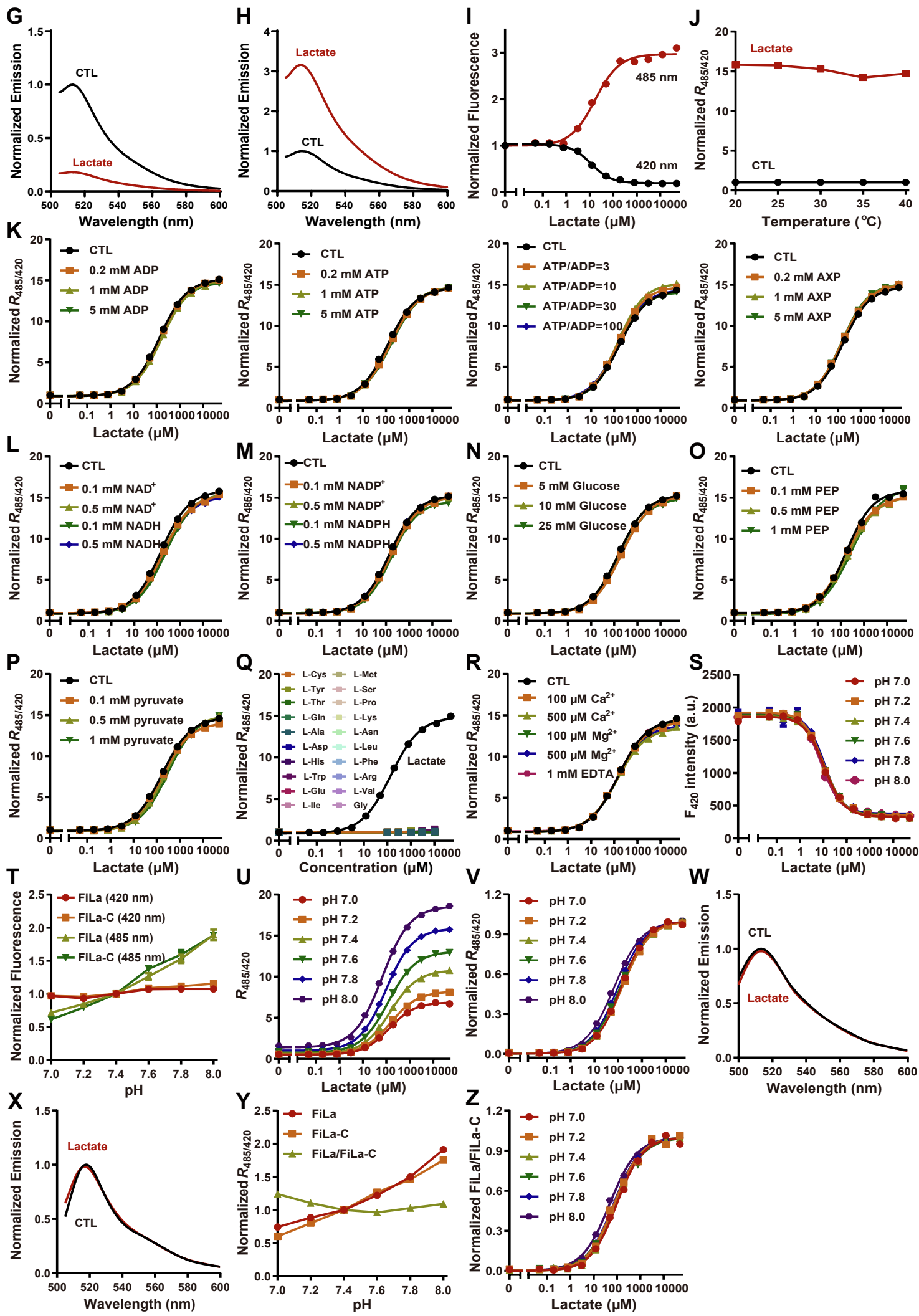
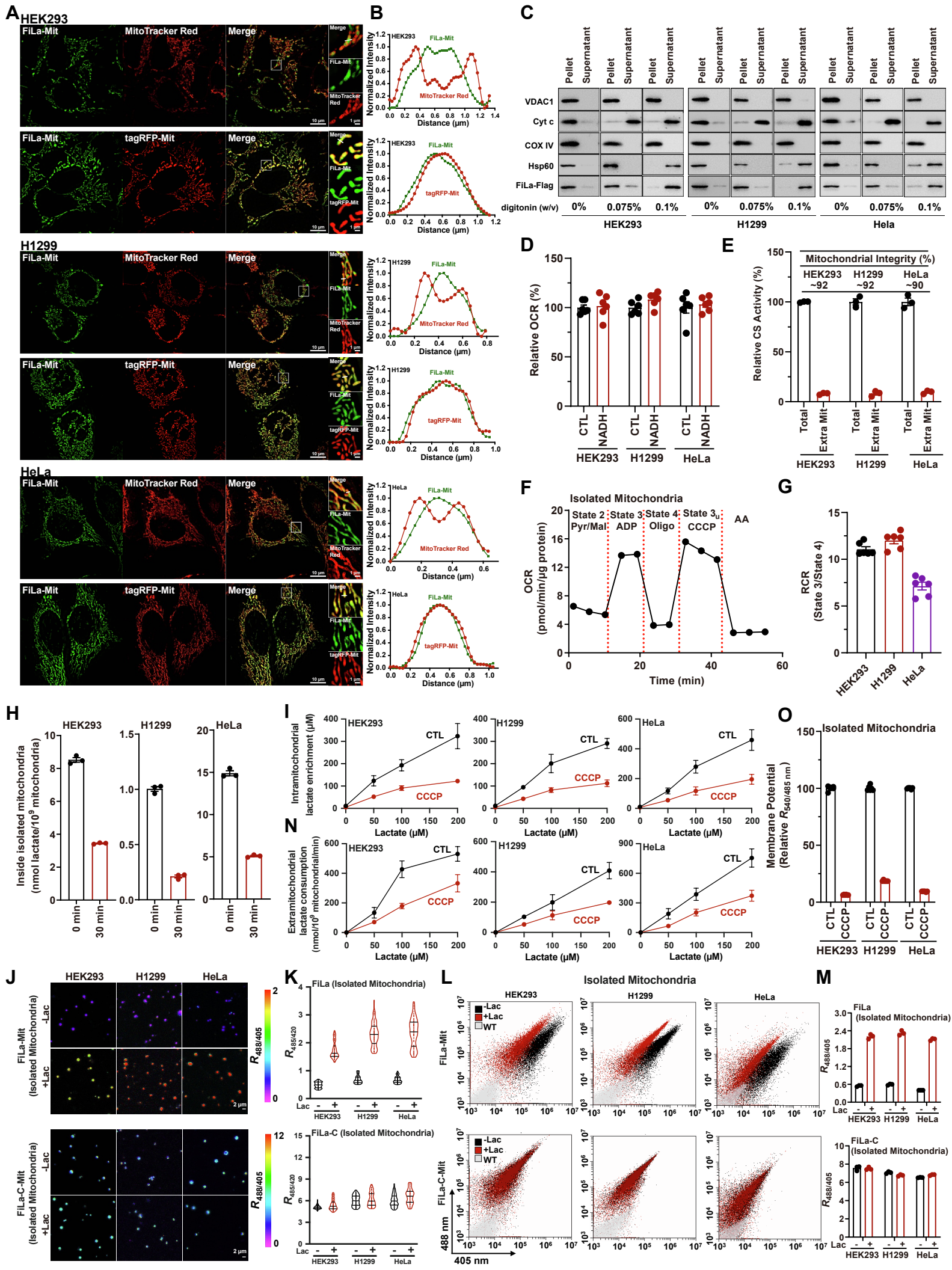


Figure S1, related to Figure 1. Design and engineering of lactate sensors. (A) Schematic model for ninety LldR and cpYFP chimeras. Two different types of sensor chimeric proteins were designed. In the upper panel, cpYFP was inserted between two complete (1-258) or truncated (80-258) subunits of LldR. A series of short polypeptide linkers between LldR (80-258) and cpYFP were created (a total of 19 sensor chimeras). In the lower panel, cpYFP was inserted into flexible linker 58-60 regions, 65-68 regions, 59-78 regions and 72-78 regions of complete LldR with DNA-binding domain or linker 93-97 regions, 119-121 regions, 137-141 regions, 158-161 regions, 186-191 regions, 208-210 regions and 230-232 regions of truncated LldR without the DNA-binding domain. Please also see Figure S1B for fluorescence properties of 90 sensor chimeras. **(B)** Fluorescence response of ninety chimeras in the presence of 10 mM lactate. **(C)** Normalized fluorescence change of Y186/P189 truncations in response to 10 mM lactate (n=3). **(D)** High throughput screening of a library of random mutants (~700 variants) targeting the residues Pro189 and Pro190 based on the M185/P189 chimera. **(E)** Fluorescence titration curves of P189C/P190D (CD), P189M/P190D (MD), P189H/P190D (HD), and P189F/P190D (FD) (n=3). **(F)** Heatmap of site-saturation mutants at the residue M185, based on the CD, MD, HD, and FD chimera. **(G and H)** Emission spectra of purified FiLa in the control condition (black), and saturated lactate (dark red), normalized to the peak intensity in the control condition. Excitation was fixed at 420 nm (G) and 490 nm (H), respectively. **(I)** Fluorescence intensities of FiLa with excitation at 485 nm or 420 nm in the presence of lactate, and emission at 528 nm. Data are normalized to the fluorescence in the absence of lactate (n=3). **(J)** Fluorescence response of FiLa to 50 mM lactate at various temperatures (n=3). **(K)** Fluorescence of FiLa plotted against lactate at the indicated ADP, ATP, ATP:ADP (ratios of physiological conditions; the total adenine nucleotide concentration was 1 mM), or AXP (ATP:ADP=100:1), normalized to the initial value (n=3). **(L-P)** Fluorescence of FiLa plotted against lactate at the indicated NAD⁺, NADH (L) or NADP⁺, NADPH (M), glucose (N), phosphoenolpyruvate (PEP, O), or pyruvate (P), normalized to the initial value (n=3). **(Q)** Fluorescence response of FiLa in the presence of lactate, and 20 amino acids, normalized to

the initial value (n=3). **(R)** Fluorescence of FiLa plotted against lactate at the indicated Ca^{2+} , Mg^{2+} , or EDTA, normalized to the initial value (n=3). **(S)** FiLa F_{420} intensity (arbitrary units, a.u.) as a function of lactate concentration at the indicated pH. **(T)** Fluorescence intensities of FiLa and FiLa-C with excitation at 420 nm or 485 nm, and emission at 528 nm. Data are normalized to the fluorescence at pH 7.4 (n=3). **(U and V)** Un-normalized (U) and normalized (V) ratio of FiLa fluorescence excited at 485 nm and 420 nm at the indicated pH plotted against lactate. For (V), the data were normalized to the 0-1 scale to demonstrate that FiLa's K_d is more pH resistant (n=3). **(W and X)** Emission spectra of purified FiLa-C in the control condition (black), and 10 mM lactate (dark red), normalized to the peak intensity in the control condition. Excitation was fixed at 420 nm (W) and 490 nm (X), respectively. **(Y)** pH-dependence of the excitation ratio of FiLa and FiLa-C. Data are normalized to the fluorescence at pH 7.4 (n=3). **(Z)** $R_{\text{FiLa}/\text{FiLa-C}}$ at the indicated pH plotted against lactate, the data were normalized to the 0-1 scale (n=3). All data are presented as mean \pm SEM.



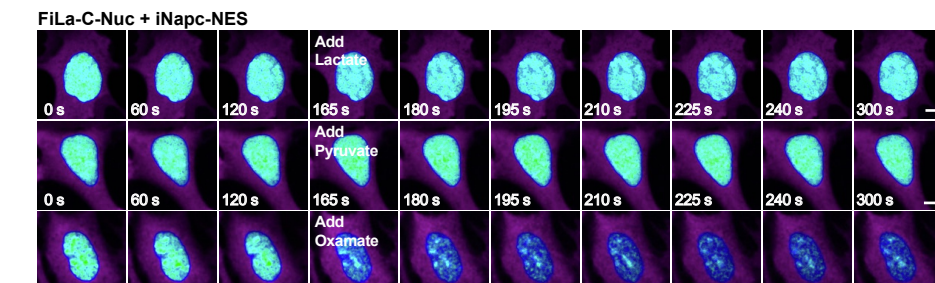
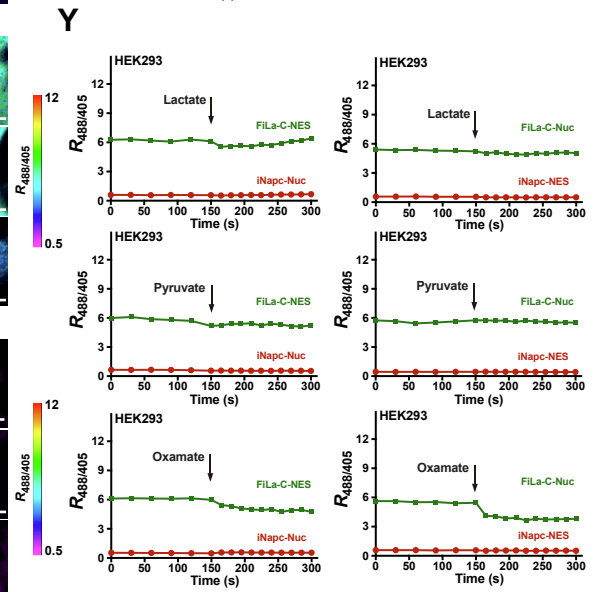
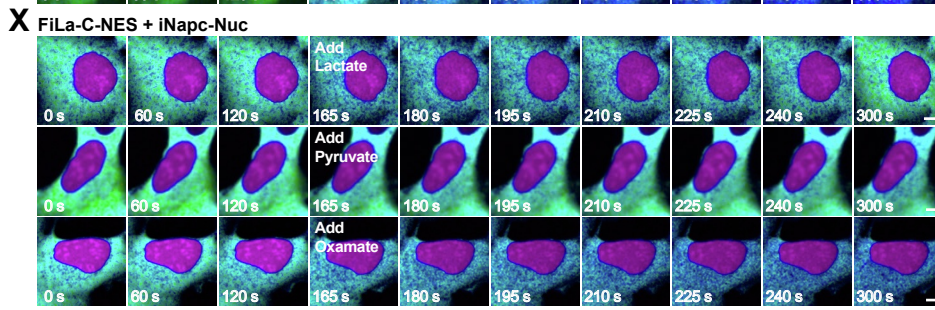
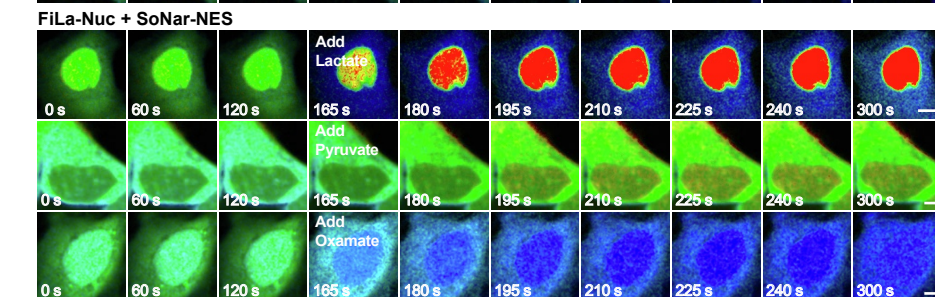
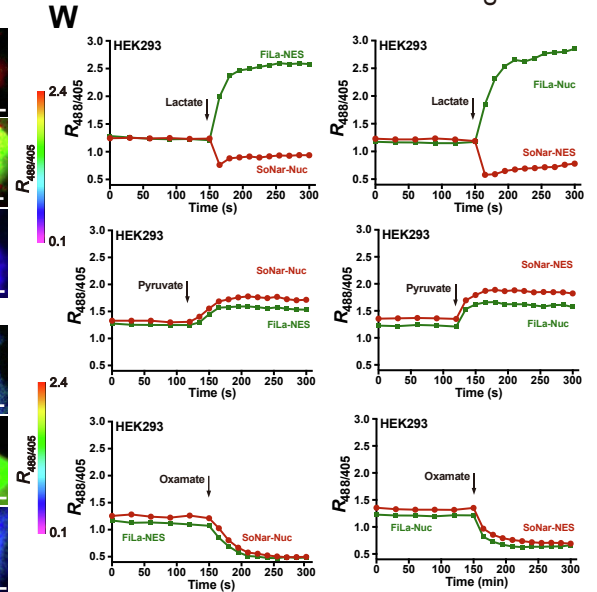
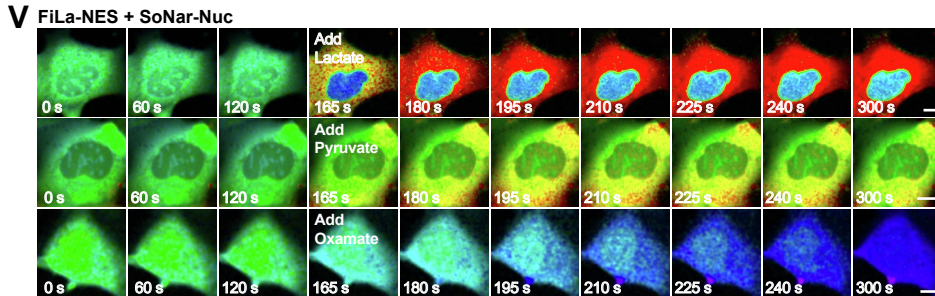
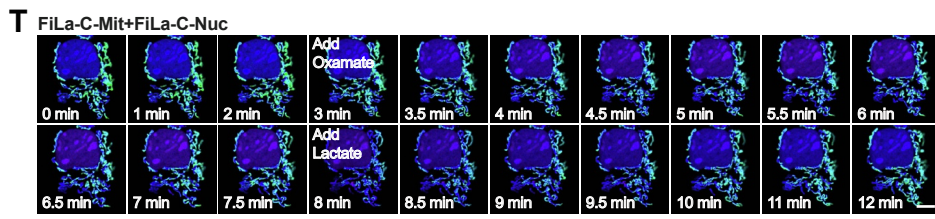
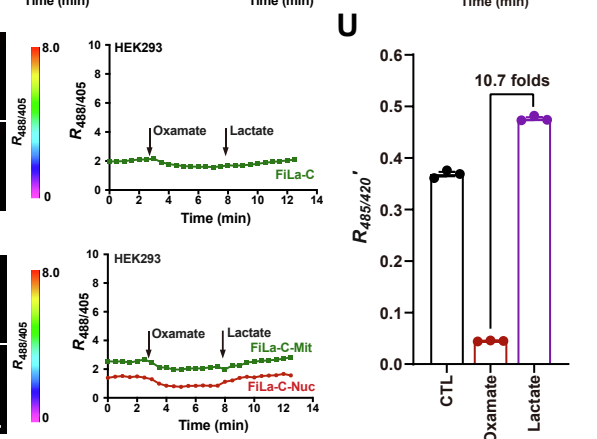
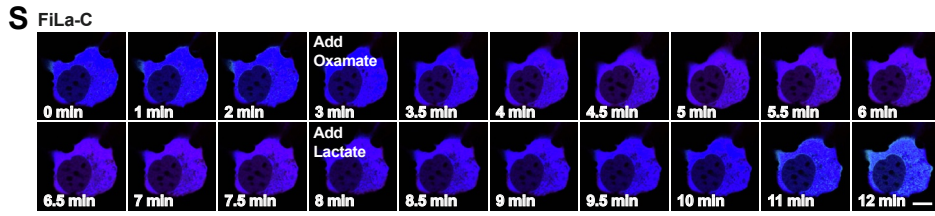
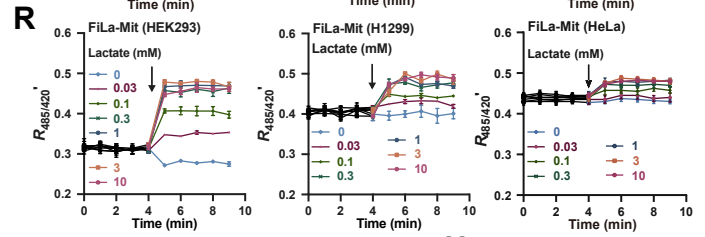
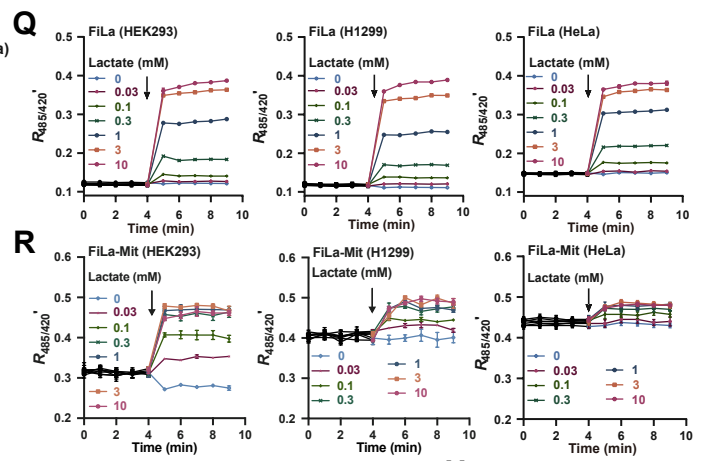
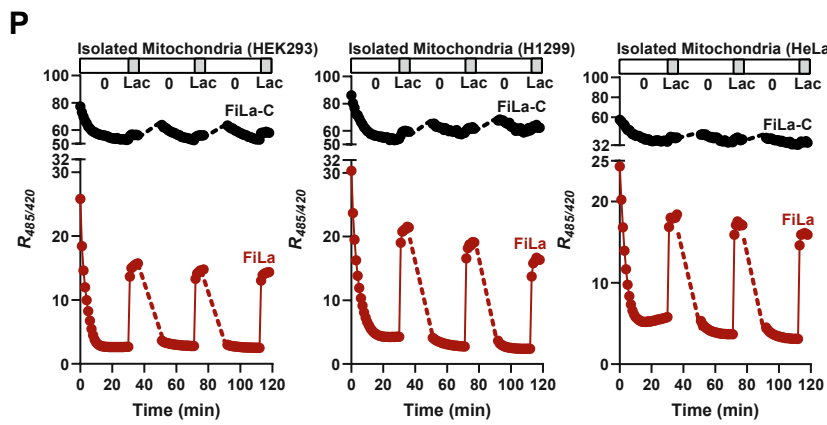


Figure S2, related to Figure 2. Imaging and quantifying lactate metabolism in living cells. (A and B)

Fluorescence images (A) and plot profile (B) of HEK293, H1299 or HeLa cells expressing FiLa-Mit co-labeled with MitoTracker Red or tagRFP-Mit. Data have been normalized to the maximum intensity of each individual color channel. Scale bars, 10 μm or 1 μm . **(C)** Submitochondrial localization of the FiLa-Mit sensor was examined by subfractionation. Mitochondria preparations from HEK293, H1299 and HeLa cells expressing the FiLa-Mit sensor were incubated with 0.075% digitonin to rupture the outer membrane, or 0.1% digitonin to disrupt both the outer and the inner membranes. All fractions obtained were then tested by immunoblotting for VDAC1 as a marker for the outer-membrane fraction, COX IV for the inner-membrane fraction, cytochrome c for the inter-membrane space fraction, and Hsp60 for the matrix fraction. **(D)** Oxygen consumption rates (OCRs) of isolated mitochondria of three cell types in the absence or presence of NADH (1 mM) (n=6). **(E)** Quantitative analysis of citrate synthase activity in mitochondria preparations from three different cells (n=3). **(F)** Seahorse coupling assay of the freshly isolated mitochondria. Pyruvate (Pyr, 10 mM) and malate (Mal, 5 mM) were used as substrates to feed electrons to complex I and basal (state 2) respiration was measured. State 3 respiration was determined in the presence of ADP (4 mM). Oligomycin (Oligo, 3.5 μM) addition blocked ATP synthase and evoked state 4 respiration. State 3_u respiration was measured in the presence of the uncoupler CCCP (4 μM). Antimycin A (AA, 4.5 μM) was injected to inhibit complex III (n=6). **(G)** Respiration control ratio (RCR, State 3/State 4) of three cell types (n=6). **(H)** Lactate levels of isolated mitochondria after 30 min incubation, as measured by the biochemical assay (n=3). **(I)** Intramitochondrial lactate enrichment of isolated mitochondria from three cell types treated with or without 10 μM CCCP at the indicated exogenous lactate (n=4). **(J-M)** Fluorescence imaging (J and K) and flow cytometric analysis (L and M) of isolated mitochondria from three cells expressing FiLa-Mit or FiLa-C-Mit in response to 1 mM lactate. For J, scale bars, 2 μm . For K, n=100. For M, n=3. **(N)** Extramitochondrial lactate consumption of isolated mitochondria from three cell types treated with or without 10 μM CCCP at the indicated exogenous

lactate (n=4). **(O)** Mitochondrial membrane potential of isolated mitochondria from three cells treated with or without CCCP (n=6). **(P)** Kinetics of FiLa and FiLa-C fluorescence in isolated mitochondria of three cell types in response to successive addition or removal of 1 mM lactate (n=5). **(Q and R)** Kinetics of FiLa (Q) or FiLa-Mit (R) fluorescence response in HEK293, H1299, and HeLa cells treated with exogenous lactate (n=4). FiLa's fluorescence was corrected by FiLa-C. **(S and T)** Fluorescence images (left) and quantification (right) of FiLa-C expressed in the cytosol (S) or nucleus and mitochondria (T) of HEK293 cells. Cells were treated with 5 mM oxamate followed with 2 mM lactate successively at the indicated time. Scale bars, 10 μ m. **(U)** Effects of oxamate (10 mM) and lactate (10 mM) on mitochondrial lactate levels in HEK293 cells measured by FiLa. FiLa's fluorescence ratios were corrected by FiLa-C (n=3). **(V and W)** Fluorescence images (V) and quantification (W) of HEK293 cells simultaneously expressing FiLa in the cytosol and SoNar in the nucleus (V, upper; W, left), or FiLa sensor in the nucleus and SoNar in the cytosol (V, lower; W, right). Cells were treated with 2 mM lactate, 0.5 mM pyruvate, or 5 mM oxamate at the indicated time, respectively. Scale bars, 10 μ m. **(X and Y)** Fluorescence images (X) and quantification (Y) of HEK293 cells simultaneously expressing FiLa-C in the cytosol and iNapc in the nucleus (X, upper; Y, left), or FiLa-C sensor in the nucleus and iNapc in the cytosol (X, lower; Y, right). Cells were treated with 2 mM lactate, 0.5 mM pyruvate, or 5 mM oxamate at the indicated time, respectively. Scale bars, 10 μ m. Data are the mean \pm SEM (D-I, M-R, U) or mean \pm SD (K).

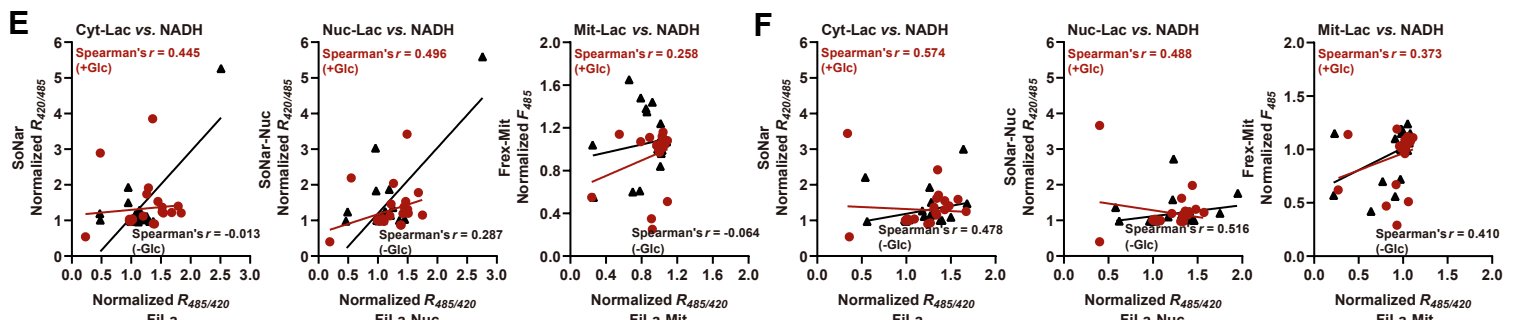
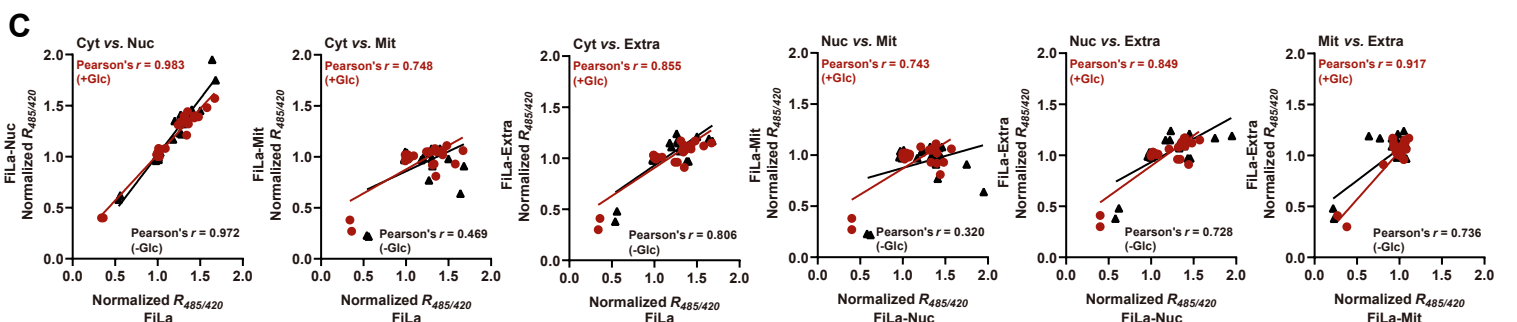
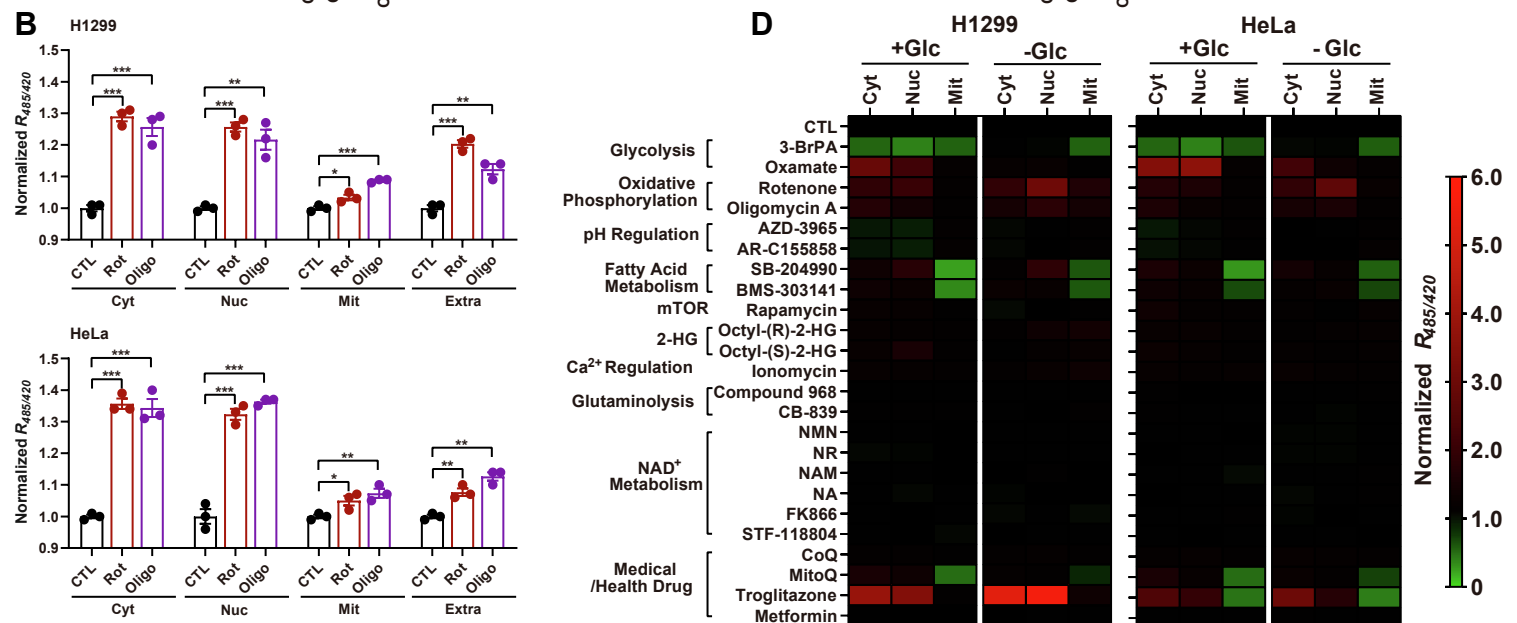
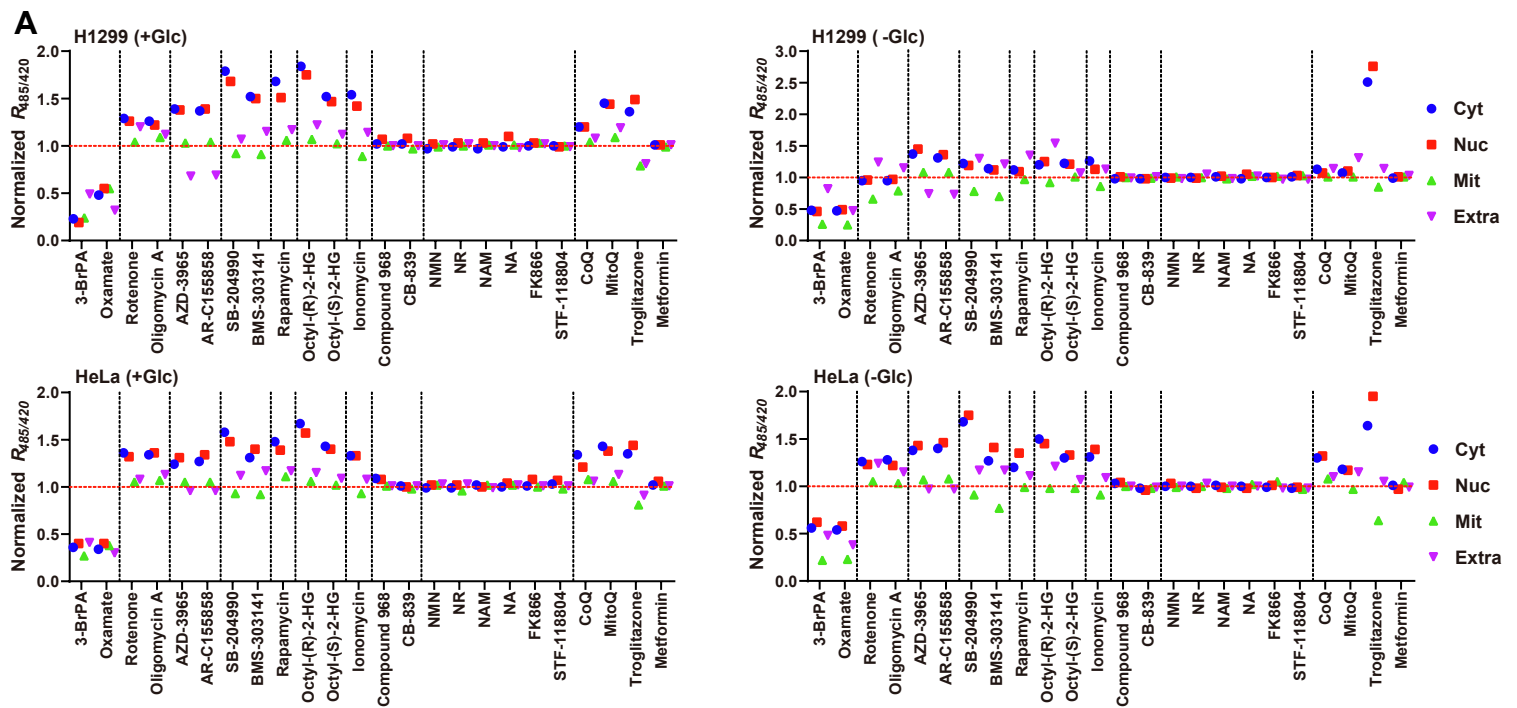


Figure S3, related to Figure 3. Lactate as a key hub sensing various metabolic activities. (A) Effects of 24 metabolic modulators targeting 10 typical metabolic pathways on subcellular lactate levels in two typical cancer cell lines under glucose-fed or glucose-deprived conditions, presented as scatter plots. Different metabolic pathways shown in Figure 3B were divided by black dashed lines. Individual dots represent average of 3 independent measurements by FiLa for each sample. Data are from Table S3. **(B)** Effects of rotenone (Rot) and oligomycin (Oligo) on subcellular lactate levels in H1299 and HeLa cells measured by FiLa (n=3). Data are from Figure 3B and Table S3. **(C)** Pearson correlation analysis of lactate levels between every two subcellular compartments in glucose-fed (dark red) or glucose-deprived (black) HeLa cells. Data are from Table S3. **(D)** Effects of 24 metabolic modulators targeting 10 typical metabolic pathways on subcellular (cytosol, nucleus, and mitochondria) NADH metabolism in two cancer cell lines. Experiments were conducted in 25 mM glucose (glucose-fed) or 0 mM glucose (glucose-deprived) condition. SoNar (cytosol and nucleus) or Frex (mitochondria) fluorescence response was corrected by iNapc or cpYFP, respectively. Data are normalized to the control group and results are shown as a heatmap. Data are from Table S4. **(E and F)** Spearman correlation analysis between lactate and NADH levels in three subcellular compartments in glucose-fed (dark red) or glucose-deprived (black) H1299 (E) or HeLa (F) cells. Data are from Table S3 and Table S4.

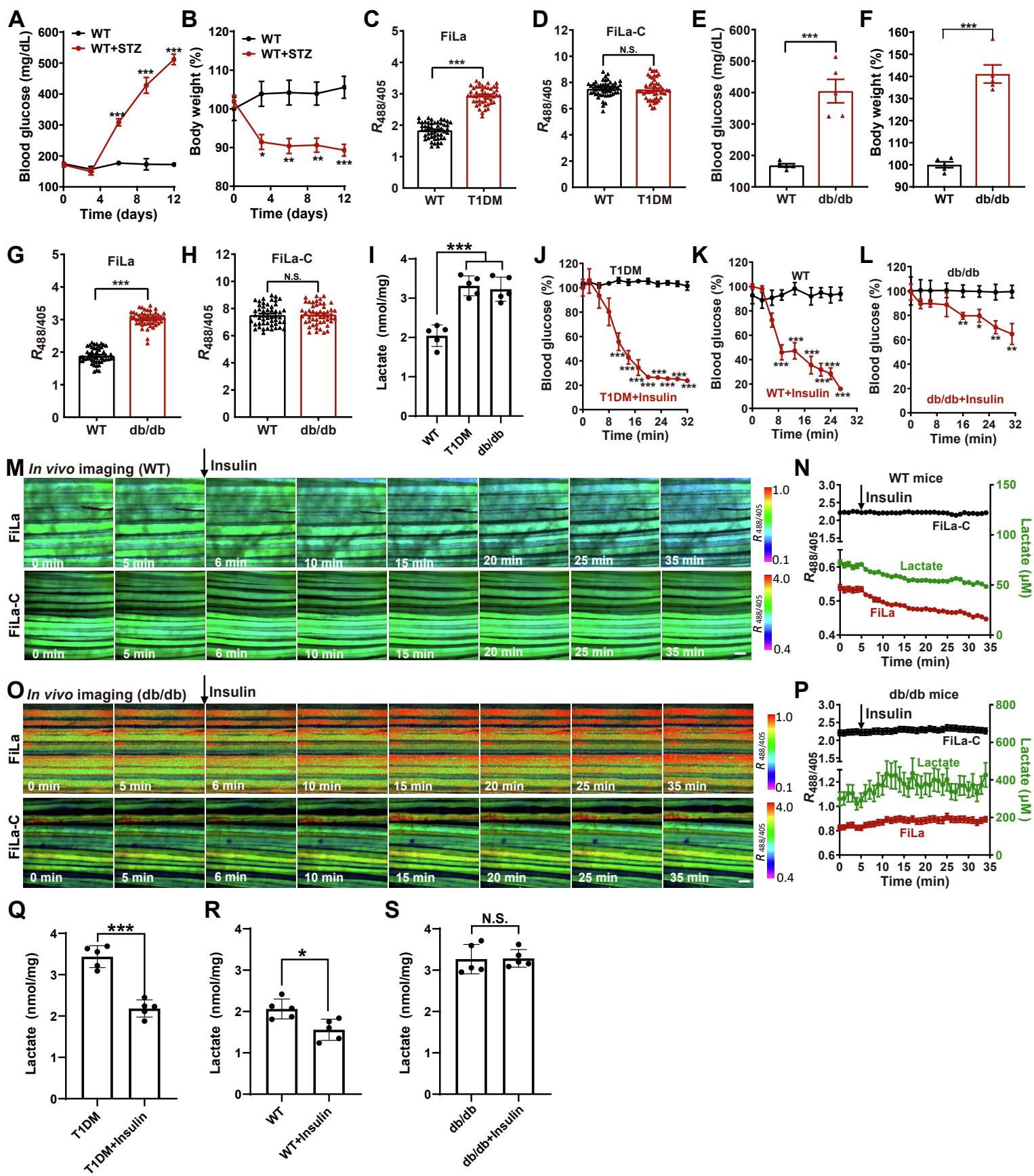


Figure S4, related to Figure 4. Lactate metabolism in live T1DM and T2DM mice. (A and B) Blood glucose (A) and body weight (B) monitoring of streptozotocin (STZ)-induced T1DM mice and WT mice (n=5 mice for WT and T1DM). **(C and D)** Quantification of FiLa (C) and FiLa-C (D) in muscle tissue of living T1DM and WT mice (n=50 muscle fibers, 5 mice). **(E and F)** Blood glucose (E) and body weight (F) monitoring of db/db mice and WT mice (n=5 mice for WT and db/db). **(G and H)** Quantification of FiLa (G) and FiLa-C (H) in muscle tissue of living db/db and WT mice (n=50 muscle fibers, 5 mice). **(I)** Lactate biochemical assay in muscle tissue of WT, T1DM and db/db mice (n=5 mice for WT, T1DM and db/db). **(J)** Percentage of blood glucose from T1DM mice by insulin therapy replotted from Figure 4J (n=4 mice for T1DM; n=6 mice for T1DM + insulin). **(K and L)** Percentage of blood glucose from WT and db/db mice by insulin therapy. Insulin sensitivity was measured by blood glucose curve, insulin (1.25 units/kg) was injected via intraperitoneal (n=5 mice for WT, WT + insulin, db/db and db/db + insulin). **(M-P)** *In vivo* fluorescence imaging (M and O) and quantification (N and P) of FiLa and FiLa-C in muscle tissue of living WT (M and N) and db/db (O and P) mice treated with insulin (n=11 muscle fibers). All fluorescence images are pseudocolored by $R_{488/405}$. Scale bars, 100 μm . **(Q-S)** Lactate biochemical assay in muscle tissue of T1DM, WT and db/db mice by insulin therapy (n=5 mice for T1DM, T1DM + insulin, WT, WT + insulin, db/db and db/db + insulin). All data are presented as mean \pm SEM. All p values were obtained using unpaired two-tailed Student's t-test. * $p < 0.05$, ** $p < 0.01$, *** $p < 0.001$. N.S., not significant.

Healthy					MIDD (m.3243A>G)					LADA					T2DM				
No.	Sex	Age	BMI (kg/m ²)	HbA _{1c} (%)	No.	Sex	Age	BMI (kg/m ²)	HbA _{1c} (%)	No.	Sex	Age	BMI (kg/m ²)	HbA _{1c} (%)	No.	Sex	Age	BMI (kg/m ²)	HbA _{1c} (%)
Healthy-1	Female	39	19.7	5.8	MIDD-1	Female	44	16	5.4	LADA-1	Female	38	22.9	8.7	T2DM-1	Female	39	21.3	6.9
Healthy-2	Female	57	21.0	5.5	MIDD-2	Female	60	19.5	6.5	LADA-2	Female	56	22.6	8.5	T2DM-2	Female	55	22.5	7.4
Healthy-3	Female	55	21.8	6	MIDD-3	Female	51	21.2	6.8	LADA-3	Female	46	26.6	6.9	T2DM-3	Female	59	20.44	7.3
Healthy-4	Female	26	19.7	5.9	MIDD-4	Female	28	23.6	7.8	LADA-4	Female	30	20.3	8.2	T2DM-4	Female	34	26.17	10.1
Healthy-5	Female	47	24.0	5.9	MIDD-5	Female	48	25.6	10.2	LADA-5	Female	47	23.3	7.3	T2DM-5	Female	42	24.3	10.3
Healthy-6	Female	33	18.7	5.4	MIDD-6	Female	30	19.8	13.9	LADA-6	Female	31	19.0	10.1	T2DM-6	Female	30	17.5	8.4
Healthy-7	Female	59	24.5	5.6	MIDD-7	Female	60	22.7	6.9	LADA-7	Female	53	17.5	10.2	T2DM-7	Female	61	21.2	13
Healthy-8	Male	44	25.2	5.7	MIDD-8	Male	46	23.3	10.3	LADA-8	Male	39	19.0	13.9	T2DM-8	Male	44	23.3	11.8
Healthy-9	Male	66	19.7	6.3	MIDD-9	Male	68	20	5.6	LADA-9	Male	58	20.5	8.4	T2DM-9	Male	70	20.24	6.7
Healthy-10	Male	56	18.5	5.4	MIDD-10	Male	60	18.2	6.3	LADA-10	Male	61	17.6	8.5	T2DM-10	Male	58	22.8	13.8
Healthy-11	Male	27	22.8	5.4	MIDD-11	Male	26	25.4	9.8	LADA-11	Male	23	20.4	7.1	T2DM-11	Male	34	26.6	9
Healthy-12	Male	39	20.4	5.8	MIDD-12	Male	33	18.3	7.1	LADA-12	Male	35	20.3	6.3	T2DM-12	Male	26	18.3	14.7
Healthy-13	Male	45	24.8	5.6	MIDD-13	Male	47	17.3	6.5	LADA-13	Male	40	17.3	11.9	T2DM-13	Male	46	26.6	11.5
Healthy-14	Male	31	22.4	5.2	MIDD-14	Male	31	18.5	8	LADA-14	Male	29	20.4	10.7	T2DM-14	Male	36	19.8	7.7
Healthy-15	Male	25	19.0	5.2	MIDD-15	Male	21	19.2	8.4	LADA-15	Male	29	21.2	11.3	T2DM-15	Male	21	32.8	12.7

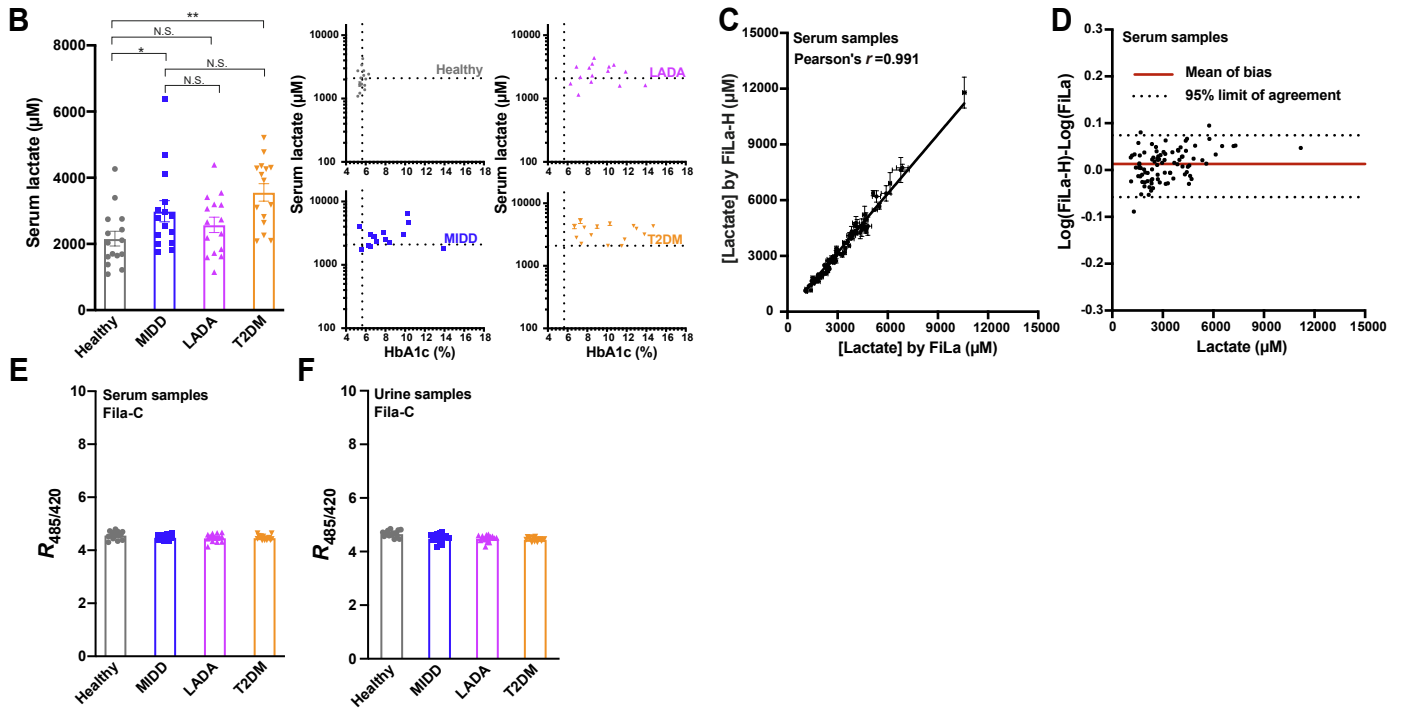


Figure S5, related to Figure 5. Lactate level in serum of patients with MIDD, LADA, and T2DM. (A) The clinical characteristics of 15 sex-, age- and BMI-matched patients with MIDD (m. 3243A>G), LADA, T2DM, and healthy people. **(B)** Serum lactate concentration of 4 groups of volunteers determined by FiLa (n=15 for each group). Data presented in bar chart or scatter plot, respectively. **(C)** Quantification of lactate in serum samples. Test results obtained by FiLa-H are plotted against results obtained by FiLa. r , correlation coefficient. **(D)** Bland-Altman analysis for serum samples measured by FiLa-H and FiLa. **(E and F)** Serum (E) or Urine (F) samples of 4 groups of volunteers determined by FiLa-C (n=15 for each group). All data are the mean \pm SEM. All p values were obtained using paired two-tailed Student's t tests. $*p < 0.05$, $**p < 0.01$. N.S., not significant.

Table S1, related to Figure 1. Primers used for FiLa sensor cloning and sequencing.

Recombinant DNA	Primer sequences for cloning	Primer sequences for sequencing
pCDFDuet-FiLa	Forward1: GTGAAGCATAGCCGTCAGCGGCTGTACAACAGCGACAACGTCTAT ATC Reverse1: TCGGTCAGTTGTGAAAAACATCATGGTTGTA CTCCAGCTTGTGCC CCAG Forward2: GTTTTTTCACAACTGACCGAACA Reverse2: CCGCTGACGGCTATGCTTCACTG	Forward: TAATACGACTCACTATAGGG Reverse: TGCTAGTTATTGCTCAGCGG
pCDFDuet-FiLa-C	Forward1: GTGAAGCATAGCCGTCAGCGGATGTACAACAGCGACAACGTCTAT ATC Reverse1: TCGGTCAGTTGTGAAAAACACCCCGTTGTA CTCCAGCTTGTGCC CCAG Forward2: GTTTTTTCACAACTGACCGAACA Reverse2: CCGCTGACGGCTATGCTTCACTG	Forward: TAATACGACTCACTATAGGG Reverse: TGCTAGTTATTGCTCAGCGG
pCDFDuet-FiLa-H	Forward1: GTGAAGCATAGCCGTCAGCGGATGTACAACAGCGACAACGTCTAT ATC Reverse1: TCGGTCAGTTGTGAAAAACATCAAAGTTGTA CTCCAGCTTGTGCC CCAG Forward2: GTTTTTTCACAACTGACCGAACA Reverse2: CCGCTGACGGCTATGCTTCACTG	Forward: TAATACGACTCACTATAGGG Reverse: TGCTAGTTATTGCTCAGCGG
pAAV-CMV-MCS-FiLa	Forward1: TGAAGCACAGCCGCCAGCGTCTGTACAACAGCGACAACGTCTATA T Reverse1: TCGGTCAGCTGGCTGAACACATCATGGTTGTA CTCCAGCTTGTGCC CCAG Forward2: GTGTT CAGCCAGCTGACCGAACA Reverse2: ACGCTGGCGGCTGTGCTT CACGC	Forward: CGCAAATGGGCGGTAGGCGTG Reverse: CATAGCGTAAAAGGAGCAACA
pAAV-CMV-MCS-FiLa-C	Forward1: TGAAGCACAGCCGCCAGCGTATGTACAACAGCGACAACGTCTATA T Reverse1: TCGGTCAGCTGGCTGAACACACCCCGTTGTA CTCCAGCTTGTGCC CCAG Forward2: GTGTT CAGCCAGCTGACCGAACA Reverse2: ACGCTGGCGGCTGTGCTT CACGC	Forward: CGCAAATGGGCGGTAGGCGTG Reverse: CATAGCGTAAAAGGAGCAACA
pcDNA3.1-Nuc-FiLa	Forward1: CGCCACCATGGATCCGATGGAGCAGAACATCGTG CAGC	Forward: CGCAAATGGGCGGTAGGCGTG

	Reverse1: TTTTGGATCAAGCTTGGATCCGGCGTTCTTCTCGCGGCTGTGT Forward2: AAGCTTGATCCAAAAAAG Reverse2: CCATCGGATCCATGGTGGCGCTAGCC	Reverse: TAGAAGGCACAGTCGAGG
pcDNA3.1-Nuc-FiLa-C	Forward1: CGCCACCATGGATCCGATGGAGCAGAACATCGTGCAGC Reverse1: TTTTGGATCAAGCTTGGATCCGGCGTTCTTCTCGCGGCTGTGT Forward2: AAGCTTGATCCAAAAAAG Reverse2: CCATCGGATCCATGGTGGCGCTAGCC	Forward: CGCAAATGGGCGGTAGGCGTG Reverse: TAGAAGGCACAGTCGAGG
pcDNA3.1-Mit-FiLa	Forward1: ATGGAGCAGAACATCGTGCAGCCG Reverse1: GGCCCTCTAGACTCGAGTTATTTGTCGTCATCATCCTT Forward2: TAACTCGAGTCTAGAGGGCCCGT Reverse2: TGCACGATGTTCTGCTCCATCGGATCCTCAGTCTTTGAAGATG	Forward: CGCAAATGGGCGGTAGGCGTG Reverse: TAGAAGGCACAGTCGAGG
pcDNA3.1-Mit-FiLa-C	Forward1: ATGGAGCAGAACATCGTGCAGCCG Reverse1: GGCCCTCTAGACTCGAGTTATTTGTCGTCATCATCCTT Forward2: TAACTCGAGTCTAGAGGGCCCGT Reverse2: TGCACGATGTTCTGCTCCATCGGATCCTCAGTCTTTGAAGATG	Forward: CGCAAATGGGCGGTAGGCGTG Reverse: TAGAAGGCACAGTCGAGG
pLVX-FiLa	Forward: CCGGTGAATTCGCCACCATGGAGCAGAACATCGTGCAGCC Reverse: GGGGCGGGATCCGCGGCCGCTTATTTGTCGTCATCATCCTTATAG	Forward: CGCAAATGGGCGGTAGGCGTG Reverse: CCTCACATTGCCAAAAGACG
pLVX-FiLa-C	Forward: CCGGTGAATTCGCCACCATGGAGCAGAACATCGTGCAGCC Reverse: GGGGCGGGATCCGCGGCCGCTTATTTGTCGTCATCATCCTTATAG	Forward: CGCAAATGGGCGGTAGGCGTG Reverse: CCTCACATTGCCAAAAGACG
pLVX-Nuc-FiLa	Forward: CCGGTGAATTCGCCACCATGGAGCAGAACATCGTGCAGCC Reverse: GGATCCGCGGCCCGGGCCCTCTAGACTCGAGTACCT	Forward: CGCAAATGGGCGGTAGGCGTG Reverse: CCTCACATTGCCAAAAGACG
pLVX-Nuc-FiLa-C	Forward: CCGGTGAATTCGCCACCATGGAGCAGAACATCGTGCAGCC Reverse: GGATCCGCGGCCCGGGCCCTCTAGACTCGAGTACCT	Forward: CGCAAATGGGCGGTAGGCGTG Reverse: CCTCACATTGCCAAAAGACG
pLVX-Mit-FiLa	Forward: CCGGTGAATTCGCCACCATGCTGTCCGTGCGCGTTGCTGC Reverse: GGGGCGGGATCCGCGGCCGCTTATTTGTCGTCATCATCCTTATAG	Forward: CGCAAATGGGCGGTAGGCGTG Reverse: CCTCACATTGCCAAAAGACG
pLVX-Mit-FiLa-C	Forward: CCGGTGAATTCGCCACCATGCTGTCCGTGCGCGTTGCTGC Reverse: GGGGCGGGATCCGCGGCCGCTTATTTGTCGTCATCATCCTTATAG	Forward: CGCAAATGGGCGGTAGGCGTG Reverse: CCTCACATTGCCAAAAGACG
pLVX-NES-FiLa	Forward: CCGGAATTCAAGCTGGCTAGCATGGCCC Reverse:	Forward: CGCAAATGGGCGGTAGGCGTG Reverse:

	GGGGCGGGATCCGCGGCCGCTTATTTGTCGTCATCATCCTTATAG	CCTCACATTGCCAAAAGACG
pLVX-NES-FiLa-C	Forward: CCGGAATCAAGCTGGCTAGCATGGCCC Reverse: GGGGCGGGATCCGCGGCCGCTTATTTGTCGTCATCATCCTTATAG	Forward: CGCAAATGGGCGGTAGGCGTG Reverse: CCTCACATTGCCAAAAGACG
pLVX-Nuc-SoNar	Forward1: CCGGTGAATTCGCCACCATGAACCGGAAGTGGGGCCTGTGCATC Reverse1: CTTTTTGGATCAAGCTTGCCCATCATCTCCTCCCGCCACTTGG Forward2: AAGCTTGATCCAAAAAAG Reverse2: GTGGCGAATTCACCGGAAATAGATCC	Forward: CGCAAATGGGCGGTAGGCGTG Reverse: CCTCACATTGCCAAAAGACG
pLVX-NES-SoNar	Forward1: GGATCCGATGGATGTCATGAACCGGAAGTGGGGCCTGTGC Reverse1: GGCGGGATCCGCGGCCGCTAGCCCATCATCTCCTCCCGCCAC Forward2: GCGGCCGCGGATCCCGCCCTCTCC Reverse2: GACATCCATCGGATCCTC	Forward: CGCAAATGGGCGGTAGGCGTG Reverse: CCTCACATTGCCAAAAGACG
pLVX-Nuc-iNapc	Forward1: CCGGTGAATTGGCTAGCATGGCGGATCCGATGAACCGGAAGTGG GGCCTGTG Reverse1: CTTTTTGGATCAAGCTTGCCCATCATCTCCTCCCGCCACTTGG Forward2: AAGCTTGATCCAAAAAAG Reverse2: CATGCTAGCCAATTCACCGGAAATAGATCC	Forward: CGCAAATGGGCGGTAGGCGTG Reverse: CCTCACATTGCCAAAAGACG
pLVX-NES-iNapc	Forward1: GGATCCGATGGATGTCATGAACCGGAAGTGGGGCCTGTGC Reverse1: GGCGGGATCCGCGGCCGCTAGCCCATCATCTCCTCCCGCCAC Forward2: GCGGCCGCGGATCCCGCCCTCTCC Reverse2: GACATCCATCGGATCCTC	Forward: CGCAAATGGGCGGTAGGCGTG Reverse: CCTCACATTGCCAAAAGACG
pLVX-Mit-Frex	Forward1: TGAGGATCCGATGAATAAGGATCAATCAAAAATT Reverse1: GGGGCGGGATCCGCGGCCGCTATTTCGATTTCTCTAAAAGT	Forward: CGCAAATGGGCGGTAGGCGTG Reverse: CCTCACATTGCCAAAAGACG
pLVX-Mit-cpYFP	Forward1: CAAAGACTGAGGATCCGATGTACAACAGCGACAACGTCTATATC Reverse1: GCGGGATCCGCGGCCGCTTAGTTGTAAGCTTGTGCCCCAGG Forward2: GCGGCCGCGGATCCCGCCCTCTC Reverse2: CGGATCCTCAGTCTTTGAAGATG	Forward: CGCAAATGGGCGGTAGGCGTG Reverse: CCTCACATTGCCAAAAGACG
pLVX-Mit-TagRFP	Forward1: GCAATGATGCTACATTTAAGGATCCGATGTCTGAGCTGATTAAG GAGAACATGCAC Reverse1: GGGGAGGGAGAGGGGCGGGATCCGCGGCCGCTTATTTGTGCCCC AGTTTGCTAGGG	Forward: CGCAAATGGGCGGTAGGCGTG Reverse: CCTCACATTGCCAAAAGACG

Table S2, related to Figure 1. Properties of FiLa sensors.

Sensor	Lactate	λ_{abs} (ϵ)	λ_{em} (QY)	Brightness ($\epsilon \cdot \text{QY}$)	K_d (μM)
FiLa	-	425 (22900)	514 (0.31)	7099	~130
		490 (4900)	514 (0.22)	1078	
	+	425 (15300)	514 (0.08)	1224	
		490 (23600)	514 (0.11)	2596	
FiLa-H	-	422 (31800)	513 (0.32)	10176	~20
		504 (1900)	520 (0.22)	418	
	+	422 (29000)	513 (0.07)	2030	
		504 (9600)	520 (0.39)	3744	
FiLa-C	-	415 (17000)	513 (0.03)	510	∞
		501 (10300)	519 (0.19)	1957	

Note: Photophysical properties of FiLa sensors with or without lactate were measured at room temperature. Extinction coefficients (ϵ , $\text{M}^{-1}\cdot\text{cm}^{-1}$) were calculated from absorbance (abs) spectra. The quantum yields of FiLa sensors were measured against EGFP. Brightness is defined as the product of extinction coefficient and quantum yield.

Table S3, related to Figure 3. Atlas of subcellular lactate metabolism.

Metabolic Pathway	Target	Drug Name	Conc. (μM)	H1299+Glc				H1299-Glc				HeLa+Glc				HeLa-Glc			
				Cyt	Nuc	Mit	EC	Cyt	Nuc	Mit	EC	Cyt	Nuc	Mit	EC	Cyt	Nuc	Mit	EC
Glycolysis	HK II	3-BrPA	500	0.23	0.19	0.24	0.49	0.48	0.46	0.26	0.82	0.36	0.40	0.27	0.41	0.56	0.62	0.22	0.48
	LDH	Oxamate	10000	0.48	0.55	0.55	0.32	0.47	0.49	0.25	0.47	0.34	0.40	0.38	0.30	0.54	0.58	0.23	0.38
ETC	Complex I	Rotenone	10	1.29	1.26	1.04	1.20	0.95	0.96	0.66	1.24	1.36	1.32	1.05	1.08	1.26	1.23	1.05	1.24
	Complex V	Oligomycin A	5	1.26	1.22	1.09	1.12	0.95	0.97	0.79	1.15	1.34	1.36	1.07	1.13	1.28	1.22	1.03	1.15
pH Regulation	MCT1	AZD-3965	2	1.39	1.38	1.03	0.68	1.37	1.45	1.08	0.74	1.24	1.31	1.05	0.96	1.38	1.43	1.07	0.97
	MCT1/2	AR-C155858	2	1.37	1.39	1.04	0.69	1.31	1.36	1.08	0.73	1.27	1.34	1.05	0.96	1.40	1.46	1.08	0.97
Fatty Acid Metabolism	ACLY	SB-204990	50	1.79	1.68	0.92	1.07	1.22	1.19	0.78	1.30	1.58	1.48	0.93	1.12	1.68	1.75	0.91	1.17
	ACLY	BMS-303141	10	1.52	1.50	0.91	1.15	1.14	1.12	0.70	1.21	1.31	1.40	0.92	1.17	1.27	1.41	0.77	1.17
mTOR	mTOR	Rapamycin	100	1.68	1.51	1.06	1.17	1.12	1.09	0.97	1.35	1.48	1.39	1.11	1.17	1.20	1.35	0.99	1.11
2-HG	ATP Synthase/mTOR	Octyl-(R)-2-HG	500	1.84	1.75	1.07	1.22	1.20	1.25	0.92	1.54	1.67	1.57	1.06	1.15	1.50	1.45	0.98	1.21
	ATP Synthase/mTOR	Octyl-(S)-2-HG	500	1.52	1.47	1.02	1.12	1.22	1.21	1.01	1.07	1.43	1.40	1.02	1.09	1.30	1.33	0.98	1.07
Ca ²⁺ Regulation	Calcium Ionophore	Ionomycin	2	1.54	1.42	0.89	1.14	1.26	1.13	0.86	1.13	1.33	1.33	0.93	1.08	1.31	1.39	0.91	1.09
Glutaminolysis	GLS	Compound 968	10	1.02	1.07	1.00	1.00	0.98	1.01	1.00	0.99	1.09	1.08	1.01	1.01	1.03	1.04	1.00	1.00
	GLS	CB-839	5	1.02	1.08	0.97	1.00	0.98	0.98	0.99	1.01	1.01	1.00	0.98	1.01	0.98	0.96	0.98	0.99
NAD ⁺ Metabolism	NAD ⁺ Precursor	NMN	500	0.97	1.02	0.99	1.01	1.00	0.99	1.01	0.98	0.99	1.02	1.02	1.03	1.00	1.03	0.99	1.00
	NAD ⁺ Precursor	NR	500	0.99	1.03	1.00	1.02	1.00	0.99	1.00	1.05	0.99	1.02	0.96	1.03	1.00	0.98	1.00	1.03
	NAD ⁺ Precursor	NAM	500	0.97	1.03	1.01	1.00	1.01	1.02	0.98	0.98	1.02	1.00	1.02	0.99	1.01	0.99	0.98	1.00
	NAD ⁺ Precursor	NA	500	0.99	1.10	1.01	0.98	0.98	1.05	1.02	1.02	1.00	1.04	1.02	1.02	1.00	0.98	1.02	1.00

	NAMPT	FK866	0.01	1.00	1.03	1.03	1.02	1.00	1.00	1.02	0.97	1.01	1.08	1.00	1.01	0.99	1.01	1.05	0.98
	NAMPT	STF-118804	0.02	1.00	0.99	1.00	0.99	1.01	1.03	1.03	0.97	1.03	1.07	0.98	1.01	0.98	0.99	0.97	0.98
Medical/health Drug	Essential Cofactor of ETC	CoQ	100	1.20	1.20	1.04	1.08	1.13	1.07	1.01	1.14	1.34	1.21	1.08	1.06	1.30	1.32	1.08	1.10
	Mitochondria-targeted Antioxidant	MitoQ	10	1.45	1.44	1.09	1.19	1.07	1.10	1.01	1.31	1.43	1.38	1.06	1.13	1.18	1.17	0.97	1.15
	Anti-diabetes Medicine	Troglitazone	100	1.36	1.49	0.79	0.81	2.51	2.76	0.85	1.14	1.35	1.44	0.81	0.91	1.64	1.95	0.64	1.05
	Anti-diabetes Medicine	Metformin	10000	1.01	1.01	0.99	1.01	0.99	1.01	1.01	1.03	1.02	1.06	1.01	1.01	1.01	0.97	1.04	0.99

Data are from normalized quantification of Fila fluorescence corrected by Fila-C to the untreated control group. Abbreviations: HK II, hexokinase II; LDH, lactate dehydrogenase; ETC, electron transport chain; MCT1/2, monocarboxylate transporter 1/2; ACLY, ATP citrate lyase; 2-HG, 2-hydroxyglutarate; GLS, glutaminase; NMN, nicotinamide mononucleotide; NR, nicotinamide riboside; NAM, nicotinamide; NA, nicotinic acid; NAMPT, nicotinamide phosphoribosyltransferase; CoQ, Coenzyme Q10; MitoQ, Mitoquinone.

Table S4, related to Figure S3. Atlas of subcellular NADH metabolism.

Metabolic Pathway	Target	Drug Name	Conc. (μM)	H1299+Glc			H1299-Glc			HeLa+Glc			HeLa-Glc		
				Cyt	Nuc	Mit	Cyt	Nuc	Mit	Cyt	Nuc	Mit	Cyt	Nuc	Mit
Glycolysis	HK II	3-BrPA	500	0.54	0.40	0.55	1.01	0.98	0.55	0.54	0.40	0.62	0.97	0.98	0.57
	LDH	Oxamate	10000	2.89	2.19	1.14	1.19	1.24	1.04	3.44	3.66	1.14	2.21	1.36	1.15
ETC	Complex I	Rotenone	10	1.91	2.04	1.10	1.93	3.03	1.65	1.71	1.62	1.12	1.93	2.72	1.24
	Complex V	Oligomycin A	5	1.74	1.46	1.08	1.50	1.83	1.48	1.62	1.26	1.10	1.51	1.58	1.11
pH Regulation	MCT1	AZD-3965	2	0.90	0.87	1.12	0.97	1.03	1.07	0.90	0.97	1.08	1.00	1.02	1.06
	MCT1/2	AR-C155858	2	0.91	0.87	1.16	0.97	1.00	1.07	0.93	0.97	1.05	1.00	1.00	1.15
Fatty Acid	ACLY	SB-204990	50	1.40	1.78	0.25	1.12	1.87	0.61	1.59	1.31	0.29	1.47	1.20	0.56
Metabolism	ACLY	BMS-303141	10	1.37	1.31	0.35	1.29	1.25	0.60	1.37	1.24	0.67	1.14	1.25	0.70
mTOR	mTOR	Rapamycin	100	1.22	1.20	1.04	0.96	1.00	1.05	1.41	1.15	1.11	1.11	1.02	1.18
2-HG	ATP Synthase/mTOR	Octyl-(R)-2-HG	500	1.21	1.15	1.08	1.06	1.36	1.44	1.25	1.22	1.10	1.09	1.15	1.19
	ATP Synthase/mTOR	Octyl-(S)-2-HG	500	1.24	1.53	1.06	1.02	1.14	1.24	1.30	1.19	1.09	1.16	1.06	1.15
Ca ²⁺ Regulation	Calcium Ionophore	Ionomycin	2	1.21	1.19	1.11	1.11	1.22	1.35	1.21	1.15	1.19	1.23	1.14	1.10
Glutaminolysis	GLS	Compound 968	10	1.02	1.02	1.03	0.99	0.99	1.03	1.04	1.00	1.00	1.02	1.01	1.04
	GLS	CB-839	5	1.04	1.05	1.04	0.99	1.00	1.06	1.04	1.01	1.01	1.02	0.98	0.99
NAD ⁺ Metabolism	NAD ⁺ Precursor	NMN	500	0.99	0.99	1.00	0.99	1.02	1.01	0.99	0.99	1.00	0.98	0.98	0.99
	NAD ⁺ Precursor	NR	500	0.97	0.98	1.00	0.99	1.02	0.99	1.00	1.03	1.03	0.98	0.98	1.03
	NAD ⁺ Precursor	NAM	500	1.03	1.01	1.00	1.00	1.04	1.00	0.99	1.01	0.96	1.03	1.01	1.04
	NAD ⁺ Precursor	NA	500	1.02	0.97	1.01	0.98	1.00	1.00	1.00	0.99	1.01	0.97	1.01	1.04
	NAMPT	FK866	0.01	1.02	1.00	1.02	0.97	0.99	0.96	1.02	0.99	1.04	0.98	1.00	0.99
	NAMPT	STF-118804	0.02	1.02	1.00	0.97	1.00	1.01	0.99	1.01	1.00	1.03	1.02	1.01	1.00

Medical/health Drug	Essential Cofactor of ETC	CoQ	100	1.12	1.13	1.05	1.10	1.14	1.09	1.16	1.19	1.07	1.21	1.16	1.10
	Mitochondria- targeted Antioxidant	MitoQ	10	1.53	1.38	0.51	1.17	1.07	0.84	1.55	1.20	0.51	1.27	1.10	0.72
	Anti-diabetes Medicine	Troglitazone	100	3.85	3.42	1.07	5.26	5.59	1.38	2.42	1.98	0.47	3.00	1.76	0.42
	Anti-diabetes Medicine	Metformin	10000	1.03	1.00	1.00	1.00	1.03	1.03	1.02	0.99	1.03	1.05	0.99	0.99

Data are from normalized quantification of SoNar corrected by iNapc (cytosol and nucleus) or Frex fluorescence corrected by cpYFP (mitochondria) to the untreated control group. Abbreviations: HK II, hexokinase II; LDH, lactate dehydrogenase; ETC, electron transport chain; MCT1/2, monocarboxylate transporter 1/2; ACLY, ATP citrate lyase; 2-HG, 2-hydroxyglutarate; GLS, glutaminase; NMN, nicotinamide mononucleotide; NR, nicotinamide riboside; NAM, nicotinamide; NA, nicotinic acid; NAMPT, nicotinamide phosphoribosyltransferase; CoQ, Coenzyme Q10; MitoQ, Mitoquinone.